EVOLUTION AND MASS ACCUMULATION OF THE CENOZOIC HOH XIL BASIN, NORTHERN TIBET

ZHIFEI LIU,[1,2] CHENGSHAN WANG,[2] AND HAISHENG YI[2]
[1] *Laboratory of Marine Geology, Tongji University, Shanghai 200092, P.R. China*
[2] *Institute of Sedimentary Geology, Chengdu University of Technology, Chengdu 610059, P.R. China*
e-mail: lzhifei@online.sh.cn

ABSTRACT: **This work reconstructs the depositional history and estimates the mass of sediments stored in the Hoh Xil basin, northern Tibet, the largest Cenozoic sedimentary basin in the hinterland of the Tibetan Plateau. The mass estimate is derived from over 75 geologic sites and 21 measured stratigraphic sections, with a total thickness of 13,478 m. The results show that the Hoh Xil basin underwent six stages of development from the Early Eocene to the Early Miocene, with a hiatus in sedimentation in the Late Oligocene. The Fenghuoshan Group was deposited during the first four stages 56.0–52.0, 52.0–43.0, 43.0–38.2, and 38.2–31.5 Myr; the Yaxicuo Group comprises stage 5, 31.5–30.0 Myr; the Wudaoliang Group covered the entire basin during the last stage, ~ 23.0 to ~ 16.0 Myr. The strata of the Fenghuoshan and Yaxicuo groups were strongly deformed, mainly during the Late Oligocene, whereas only minor tilting has occurred since then in the Wudaoliang Group. The depositional history indicates that the Hoh Xil basin could have been formed as a piggyback basin and that the onset of northeastward growth of the central Tibet was from the Early Eocene (about 56 Myr) to the Late Oligocene.**

The analyses of subsidence history and mass accumulation indicate that both accelerated subsidence and sudden increases of accumulation rate occurred at the four periods of about 52.0, 40.5, 34.5, and 31.5 Myr in three sub-basins and over the entire basin from the Early Eocene to the Early Oligocene. During the four periods, the deposits were either lacustrine turbidite sandstone or fan-delta conglomerate, which resulted from the tectonic movement. On the basis of the mechanism of northeastward growth of the piggyback basins and the consistency of accelerated subsidence, depositional systems, and mass accumulation, we suggest the continental collision and early uplift of the Tibetan Plateau controlled the formation and evolution of the Hoh Xil basin. The event that occurred at 52.0 Myr could represent the continental collision between India and Asia, whereas the other three events that happened during about 40–30 Myr could show the early uplift of the Tibetan Plateau. This study on sedimentary records in the Hoh Xil basin, along with widespread magmatic activity in eastern and western Tibet, suggests a diachronous uplift history for the Tibetan Plateau from east to west.

INTRODUCTION

The records preserved in sedimentary basins offer the possibility of quantifying the paleotopography z (x, y, t) at each point (x, y) of a given region at any time t in the past by using methods of mass-balance reconstruction (Hay et al. 1989; Métivier and Gaudemer 1997). A first important step towards establishing paleoelevations is to reconstitute the evolution of sedimentary basins in terms of mass accumulation (Métivier and Gaudemer 1997).

The collision between India and Asia has produced the highest and most extensive plateau on Earth since the Late Cretaceous (e.g., Jaeger et al. 1989; Rage et al. 1995) or the early Tertiary (e.g., Tapponnier et al. 1981; Patriat and Achache 1984). The uplift of the Tibetan Plateau is thought to have been one of the main contributions to Cenozoic global cooling (Ruddiman and Kutzbach 1991; Kutzbach et al. 1993; Ruddiman et al. 1997). At the northern margin of the Tibetan Plateau, mass-balance reconstructions have been successfully applied to the Tarim and Dzungar basins and the adjacent eastern Tien Shan (Métivier and Gaudemer 1997), and to the Qaidam and Hexi Corridor basins (Métivier et al. 1998). The analysis of paleotopography has proven to be a powerful tool in the study of active tectonics of uplift and deformation of the Tibetan Plateau. More recently, estimates of mass accumulation rates evaluated from 18, mostly Cenozoic, offshore sedimentary basins in Asia have been determined and allow a comparison of the relative importance of tectonic and erosion processes affecting the different mountain belts of Asia (Métivier et al. 1999). The geology of Cenozoic sedimentary basins in the hinterland of Tibet, however, was not considered and remains poorly understood.

We have reconstructed the depositional history and calculated the mass of sediment stored in the Cenozoic Hoh Xil basin, northern Tibet. The Hoh Xil basin, covering an area of 101,000 km^2 and with an average elevation of over 5,000 m, is the largest Cenozoic sedimentary basin in the hinterland of the Tibetan Plateau (Fig. 1). From the Early Eocene to the Early Miocene, a sediment succession consisting of approximately 5.4 km of fluvial mudstone, sandstone, and conglomerate and 0.3 km of limestone was deposited in the Hoh Xil basin. This sedimentary record contains significant information related to crustal shortening and early uplift of the Tibetan Plateau (Wang et al. 1999). Moreover, the sedimentary record sheds light on the events that occurred during the global cooling at the end of the Middle Eocene (around 37 Myr) and the cooling and drying event in the earliest Oligocene (around 33 Myr) (Liu and Wang 2000).

In this paper, we first explain the methods used to reconstruct the depositional history and the subsidence history of the basin and to estimate the average mass accumulation. We then describe measured stratigraphic sections, which are distributed across the entire basin. Finally, we present and discuss our results.

This work is advancing our understanding of the tectonic–sedimentary events recorded in the Cenozoic Hoh Xil basin, which have a direct relationship to the India–Asia continental collision and early uplift of the Tibetan Plateau. The results of this study support the mechanism of intracontinental subduction and northeastward growth and places the onset of northeastward growth of the central Tibet from the Early Eocene (about 56 Myr) to the Late Oligocene.

GEOLOGIC SETTING

The Hoh Xil basin is situated in the central part of the Baya Har terrane and the northern part of the Qiangtang terrane, and was formed on the Jinsha River Suture Zone (Fig. 1). The basin is bounded to the north by the Kunlun Mountains and the South Kunlun Suture Zone and to the south by the Tanggula Mountains and the Tanggula Fault.

The Cenozoic strata were originally subdivided into the Fenghuoshan Group (Early Cretaceous), the Yaxicuo Group (Oligocene), and the Wudaoliang Group (Miocene) (Bureau of Geology and Mineral Resources of Qinghai 1987). Subsequently, the age range of the Fenghuoshan Group was extended to Paleogene (Yin et al. 1990) or Cretaceous (Zhang and Zheng 1994) on the basis of a small number of fossils. More recently, detailed lithostratigraphy and magnetostratigraphy of the Fenghuoshan and Yaxicuo groups have been established with precise chronology of the sediments: the Fenghuoshan Group was deposited from 56.0 to 31.5 Myr, and the Yaxicuo Group from 31.5 to 30.0 Myr (Liu et al. 2000a) (Fig. 2). The age of the Wudaoliang Group is widely accepted as Early Miocene (~ 23.0 to ~ 16.0 Myr) on the basis of abundant fossils (Bureau of Geology and

JOURNAL OF SEDIMENTARY RESEARCH, VOL. 71, NO. 6, NOVEMBER, 2001, P. 971–984
 1527-1404/01/071-971/$03.00

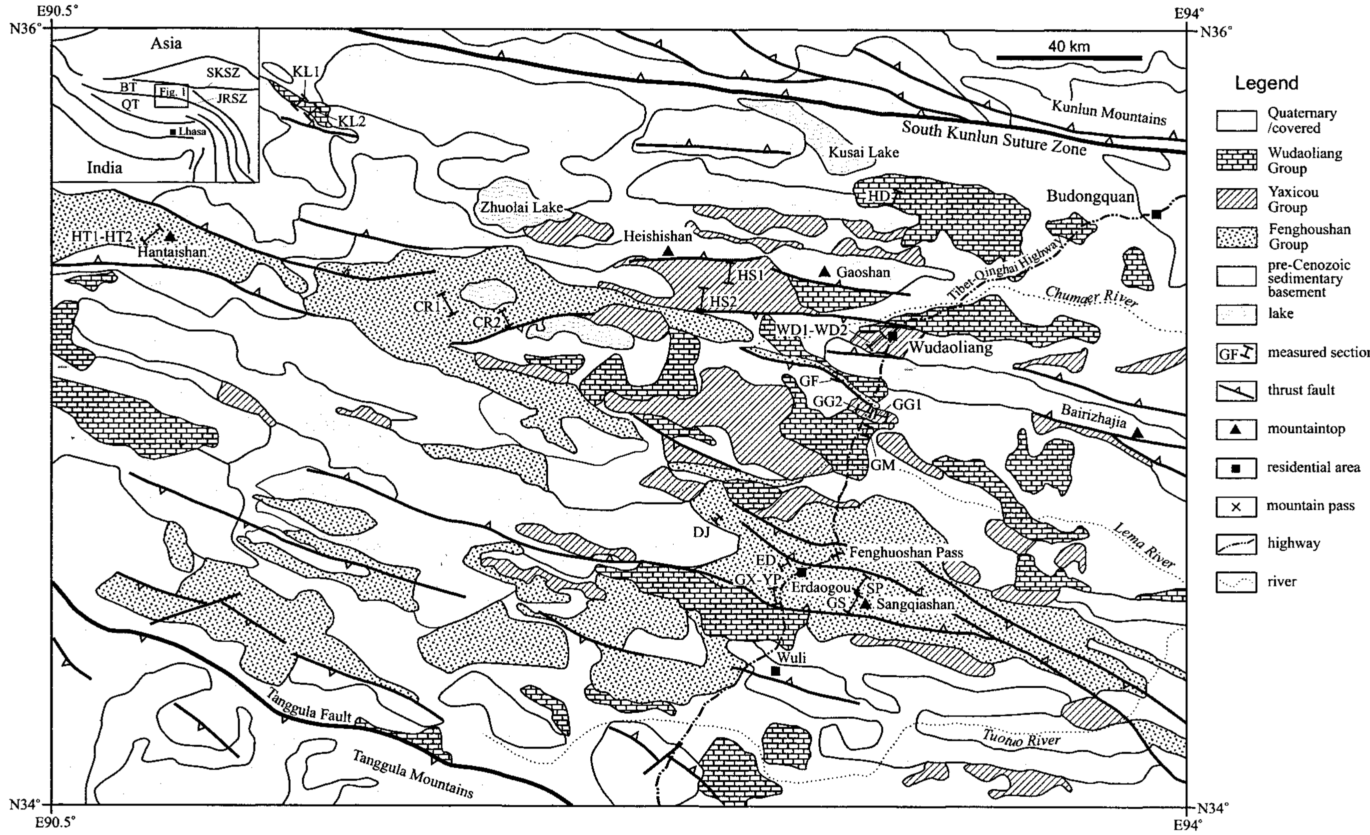

FIG. 1.—Simplified geologic map of the Hoh Xil basin, showing north and south boundaries of the basin, tectonic framework, and distribution of Cenozoic sediments and measured stratigraphic sections. Modified from Zhang and Zheng (1994). QT, Qiangtang terrane; BT, Baya Har terrane; JRSZ, Jinsha River Suture Zone; SKSZ, South Kunlun Suture Zone.

Mineral Resources of Qinghai 1991; Zhang and Zheng 1994). During the Late Oligocene, there was a depositional hiatus of some 7.0 Myr in the Hoh Xil basin. The pre-Cenozoic sedimentary basement of the Hoh Xil basin consists of Carboniferous, Permian, and Triassic slate, phyllite, metasandstone, and limestone (Fig. 1; Zhang and Zheng 1994).

A series of WNW-striking thrust faults offset both the pre-Cenozoic sedimentary basement and the Cenozoic sedimentary deposits (Fig. 1). The strata of the Fenghuoshan and Yaxicuo groups have undergone strong deformation, whereas only minor tilting has occurred in the Wudaoliang Group. The north–south crustal shortening during the Late Oligocene has been estimated at about 40% in the Fenghuoshan area (Coward et al. 1990) or 42.8% in the Wudaoliang–Fenghuoshan areas (Wang et al. 1999). Thus, deformation of the Paleogene sediments occurred mainly during the Late Oligocene. Satellite imagery interpretation, along with fieldwork, indicates that the contact between the Fenghuoshan Group and the overlying Yaxicuo Group is concordant but that the Wudaoliang Group discordantly overlies the deformed Paleogene Fenghuoshan and Yaxicuo groups.

DATA AND METHODS

This paper is based on a detailed study of outcrop stratigraphic sections and backstripping analysis of the surface stratigraphic data. Twenty-one stratigraphic sections including 11 within the Fenghuoshan Group, 6 within the Yaxicuo Group, and 4 within the Wudaoliang Group (Table 1), and over 75 geologic sites were measured and examined. The stratigraphic sections have a total thickness of 13,478 m and are distributed across the entire Hoh Xil basin, with the exception of the southwestern region because the units are poorly exposed there (Fig. 1). Correlation among the sections is based mainly on lithology. Magnetostratigraphic dating of the typical sections is modified from Liu et al. (2000a) according to the timescale of Harland et al. (1990). A total of 308 paleocurrent measurements from sedimentary structures at the stratigraphic sections and other outcrops of the Fenghuoshan and Yaxicuo groups were collected in the field using a magnetic compass. The measured structures include flutes, small-scale and large-scale cross-stratification, and pebble imbrication. The paleocurrent data, corrected for tectonic structure, have been grouped and plotted according to the stages of basin evolution.

The measured stratigraphic thickness was decompacted using the backstripping method after van Hinte (1978) and Steckler and Watts (1978). Sedimentary isopachs were reconstructed by the interpolated point method based on the corrected stratigraphic thickness and the distribution of Cenozoic sediments. We assume that the distribution of present outcrops in the field represents the original depositional ranges and that the value of depositional area margins was 0 meters. The present distribution areas are corrected using the north–south crustal shortening of 42.8% that occurred during the Late Oligocene (Table 2; Wang et al. 1999). The sediment volumes are calculated from the hypothesis of regional similarity developed by Métivier and Gaudemer (1997) and Métivier et al. (1998) based on the units of polarity chrons and sub-basins. The method of subsidence analysis is after Allen and Allen (1990) and Shao et al. (1999).

LITHOSTRATIGRAPHY

The stratigraphy of the Cenozoic Hoh Xil basin was previously studied in general, but with the Cretaceous depositional age based on a small number of fossils (Bureau of Geology and Mineral Resources of Qinghai 1987; Zhang and Zheng 1994). The detailed lithostratigraphic studies, along with

Epoch		Stratigraphy		Basin evolution	Age (Myr)	Thickness (m)		Depositional environment
Miocene	Early	Wudaoliang Group		Stage 6	~16.0 – ~23.0	370		lacustrine
Oligocene	Late	MISSING						
Oligocene	Early	Yaxicuo Group		Stage 5	30.0 – 31.5	670		lacustrine/fluvial
Eocene	Late	Fenghuoshan Group	Unit 4	Stage 4	31.5 – 38.2	4783	1396	fluvial/lacustrine
Eocene	Middle	Fenghuoshan Group	Unit 3	Stage 3	38.2 – 43.0	4783	1424	fluvial/fan-delta
Eocene	Middle	Fenghuoshan Group	Unit 2	Stage 2	43.0 – 52.0	4783	1116	lacustrine
Eocene	Early	Fenghuoshan Group	Unit 1	Stage 1	52.0 – 56.0	4783	847	fluvial/lacustrine

FIG. 2.—Stratigraphy, evolution stage, and depositional environment of Cenozoic sediments in the Hoh Xil basin. Uncertainty of measured thickness from typical stratigraphic sections is about 5%. Ages of the Fenghuoshan and Yaxicuo groups modified from Liu et al. (2000a), depositional environment after Liu and Wang (2001).

the magnetostratigraphic dating at the most favorable outcrops, are presented as follows.

The Fenghuoshan Group

The Fenghuoshan Group is situated mainly in the central to southern parts of the Hoh Xil basin (Fig. 1). Its lithostratigraphy and magnetostratigraphy were established on the basis of the typical sections (GX, YP, GS, and SP) (Fig. 3A, B; Liu et al. 2000a). The Fenghuoshan Group (Lower Eocene–Lower Oligocene) is 4,783 m thick and consists of gray-violet sandstone, mudstone, and conglomerate, intercalated gray-green Cu-bearing sandstone, dark-gray bioclastic limestone, and gray gypsum. The group was interpreted as representing fluvial, lacustrine, and fan-delta depositional environments and was subdivided into four lithological units according to facies analysis and depositional systems (Fig. 2; Liu and Wang 2001). In ascending order, these are: sandstone, mudstone, and intercalated gypsum, with a thickness of 847 m (Unit 1); alternating mudstone and sandstone with intercalated limestone, with a thickness of 1,116 m (Unit 2); sandstone and conglomerate, with a thickness of 1,424 m (Unit 3); and sandstone and mudstone, with a thickness of 1,396 m (Unit 4).

TABLE 1.—*Parameters of measured stratigraphic sections of Cenozoic sediments in the Hoh Xil basin.*

Section	Stratigraphy	Lithology	Stratifications divided	Thickness (m)	Scale
GX	FG (Unit 1 & 2)	sandstone, mudstone, gypsum	68	1740	1:100
YP	FG (Unit 2)	sandstone, mudstone, limestone	10	223	1:100
GS	FG (Unit 3)	sandstone, mudstone, conglomerate	84	1424	1:1000
SP	FG (Unit 4)	sandstone, mudstone	51	1396	1:2000
HT1	FG (Unit 1 & 2)	sandstone, mudstone, conglomerate	29	768	1:2000
HT2	FG (Unit 3)	sandstone, mudstone, conglomerate	12	396	1:2000
CR1	FG (Unit 2)	sandstone, mudstone	38	1398	1:2000
CR2	FG (Unit 3)	sandstone, mudstone	26	789	1:2000
DJ	FG (Unit 1)	sandstone, conglomerate	12	342	1:1000
ED	FG (Unit 3)	sandstone, mudstone	13	318	1:500
GF	FG (Unit 4)	sandstone, mudstone	14	494	1:100
GG2	YG	sandstone, mudstone, gypsum	77	670	1:100
GG1	YG	sandstone, mudstone, gypsum	40	196	1:500
HS1	YG	sandstone, mudstone	28	593	1:1000
HS2	YG	sandstone, mudstone, conglomerate	26	898	1:1000
WD1	YG	sandstone, conglomerate	29	287	1:500
WD2	YG	sandstone	24	382	1:500
KL1	WG	marl, mudstone, calcarenite	27	259	1:200
KL2	WG	marl, mudstone	7	85	1:200
HD	WG	marl, calcarenite, crystalline, algal lump, bioclastic limestones	24	761	1:500
GM	WG	sandstone, mudstone, conglomerate	9	59	1:200

Uncertainty of measured thickness is about 5%. FG = the Fenghuoshan Group; YG = the Yaxicuo Group; WG = the Wudaoliang Group.

In addition, seven other sections of the Fenghuoshan Group were measured to correlate with the typical sections in the entire basin (Fig. 3A, B). In the central part of the basin, the measurement of the Fenghuoshan Group is represented by the sections CR1 and CR2. In the western part of the basin, two sections, HT1 and HT2, were measured in the Hantaishan area. They are correlated to sections GX, YP, and GS, respectively (Fig. 3A, B). The Fenghuoshan Group thickens from west to east and from north to south.

The Yaxicuo Group

The Yaxicuo Group is situated mainly in the central to northern parts of the Hoh Xil basin, with some small patches in the southern part (Fig. 1). A typical lithostratigraphic section (GG2) in the southern Wudaoliang area is 670 m thick and was magnetostratigraphically dated as 31.5–30.0 Myr (Fig. 2; Liu et al. 2000a). On the basis of the typical section, the Yaxicuo Group (Lower Oligocene) consists mainly of alternating sandstone and mudstone with intercalated gray gypsum and was deposited in fluvial and lacustrine environments (Liu and Wang 2001). In the Wudaoliang area, five other sections (GG1, HS1, HS2, WD1, and WD2) were also measured to investigate changes in regional thickness and distribution. They are correlated on the basis of lithology (Fig. 3C).

The Wudaoliang Group

The Wudaoliang Group is well represented in most parts of the Hoh Xil basin, thickening from south to north. Three sections (HD, KL1, and KL2) in the north and one section (GM) in the center were measured (Fig. 1). The Wudaoliang Group consists mainly of lacustrine carbonate rock, including marl, calcarenite, algal lump limestone, bioclastic limestone, and crystalline limestone, with a thin bed of sandstone and conglomerate at the base. The group also contains minor amounts of black oil shale (Liu and Wang 1999). The correlation of the four sections is shown in Fig. 3D. They give us an average thickness of 370 m (Fig. 2).

On the basis of the lithologic units and the depositional environments of the Cenozoic sedimentary rocks, we subdivide the Cenozoic evolution of the Hoh Xil basin into six stages ranging from the Early Eocene to the Early Miocene with the Late Oligocene hiatus between stage 5 and stage 6 (Figs. 2, 3). The first four stages correspond to Units 1 to 4 of the Fenghuoshan Group. Stage 5 corresponds to the Yaxicuo Group. Stage 6 is the period of Wudaoliang Group sedimentation.

BASIN EVOLUTION AND MASS ACCUMULATION

Basin Evolution

From analysis and correlation of the measured stratigraphic sections, we assessed the evolution of sediment accumulation on the basis of the basin

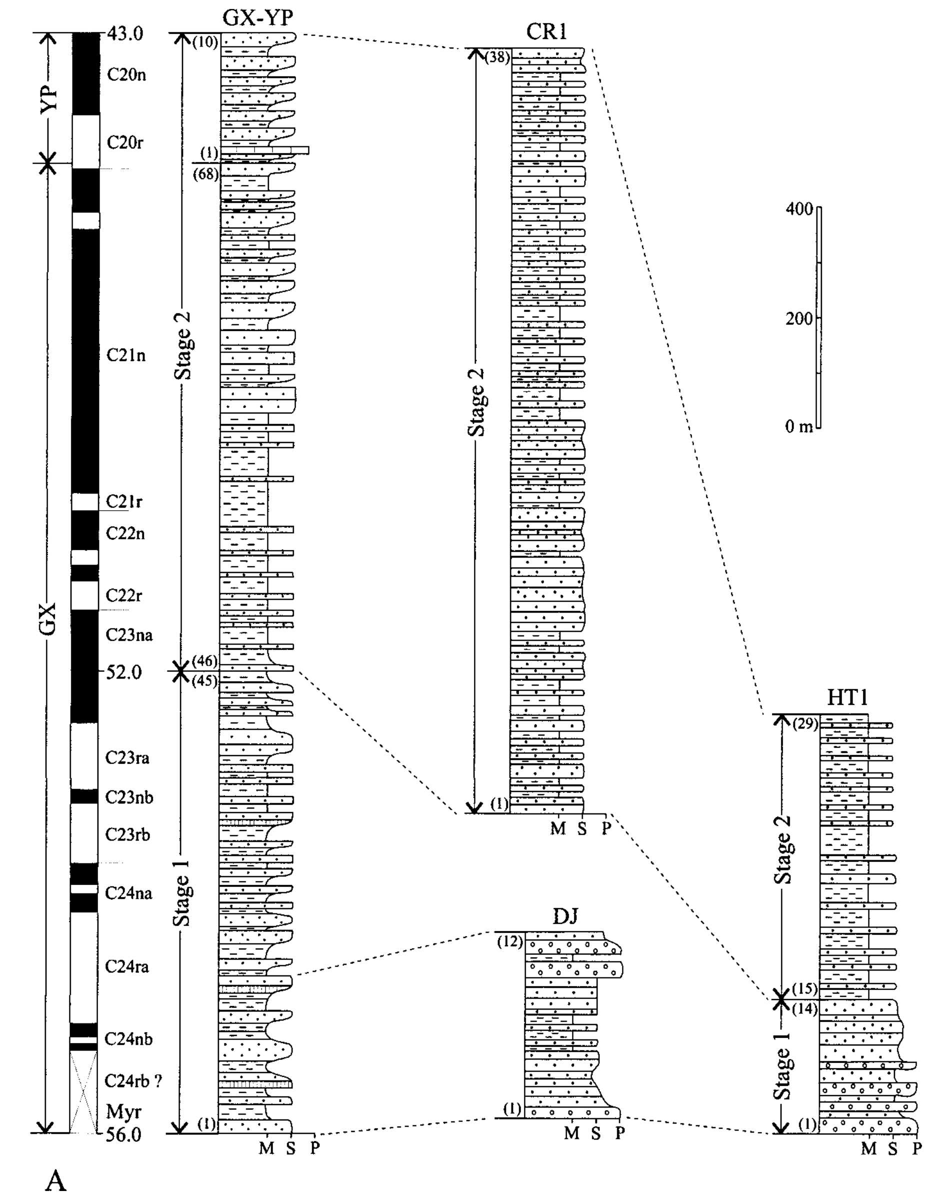

FIG. 3.—Correlation of measured stratigraphic sections of Cenozoic sediments in the Hoh Xil basin: **A)** and **B)** the Lower Eocene to Lower Oligocene Fenghuoshan Group; **C)** the Lower Oligocene Yaxicuo Group; **D)** the Lower Miocene Wudaoliang Group. The correlation among sections is based mainly on lithology. See Figure 1 for locations of sections. Polarity columns are modified from Liu et al. (2000a).

stages (Fig. 4). The Hoh Xil basin was divided into several sub-basins according to sediment thickness of the stratigraphic sections, including the Fenghuoshan sub-basin and Hantaishan sub-basin in the southern part, and the Wudaoliang sub-basin and Zhuolai Lake sub-basin in the northern part. The sedimentary isopachs were reconstructed by the interpolated point method based on the corrected stratigraphic thickness and the distribution of Cenozoic sediments.

At about 56.0 Myr, formation of the Hoh Xil basin was initiated in the foreland area of the Tanggula Mountains, probably by the collision between India and Asia (e.g., Rowley 1998). From 56.0 to 52.0 Myr, during stage 1, fan-delta to fluvial sedimentation mainly took place in the Fenghuoshan sub-basin and the Hantaishan sub-basin, with wide distribution of conglomerate (Fig. 4A). The deposits are 1,453 m thick in the Fenghuoshan sub-basin and 318 m thick in the Hantaishan sub-basin. A total of 46 paleocurrent directions in the Fenghuoshan sub-basin show NNE-directed sediment transport. In contrast, the paleocurrents indicate transport to the NW in the central part and to the SE in the western part. The various transport directions are typical of interior basin filling from surrounding mountain ranges.

From 52.0 to 43.0 Myr, during stage 2, the area of sedimentation was limited to an ESE-striking trough in the central part of the basin (Fig. 4B). The depositional environment changed from fan-delta and fluvial to lacustrine, with eastward migration of the depocenter of the Hantaishan sub-basin. The sediment thickness is up to 2,433 m in the Fenghuoshan sub-basin and up to 1,273 m in the Hantaishan sub-basin. Paleocurrent data show north-directed sediment transport.

From 43.0 to 38.2 Myr, during stage 3, the sedimentation area remained unchanged from stage 2, but both the depositional environment and paleocurrent directions changed (Fig. 4C). Fluvial to fan-delta sedimentation developed throughout the basin, with the extensive distribution of conglomerates. The Fenghuoshan sub-basin accumulated 2,139 m of sediments. The paleocurrent directions shifted from the north to the southeast and southwest in the Fenghuoshan sub-basin, to east in the eastern part, and to north in the western part of the Hantaishan sub-basin. This rotation in paleoflow directions might indicate regional tectonic activity.

From 38.2 to 31.5 Myr, during stage 4, the depocenter migrated eastward and northward and no sedimentation occurred in the Hantaishan sub-basin (Fig. 4D). The Wudaoliang sub-basin was formed in the north margin of

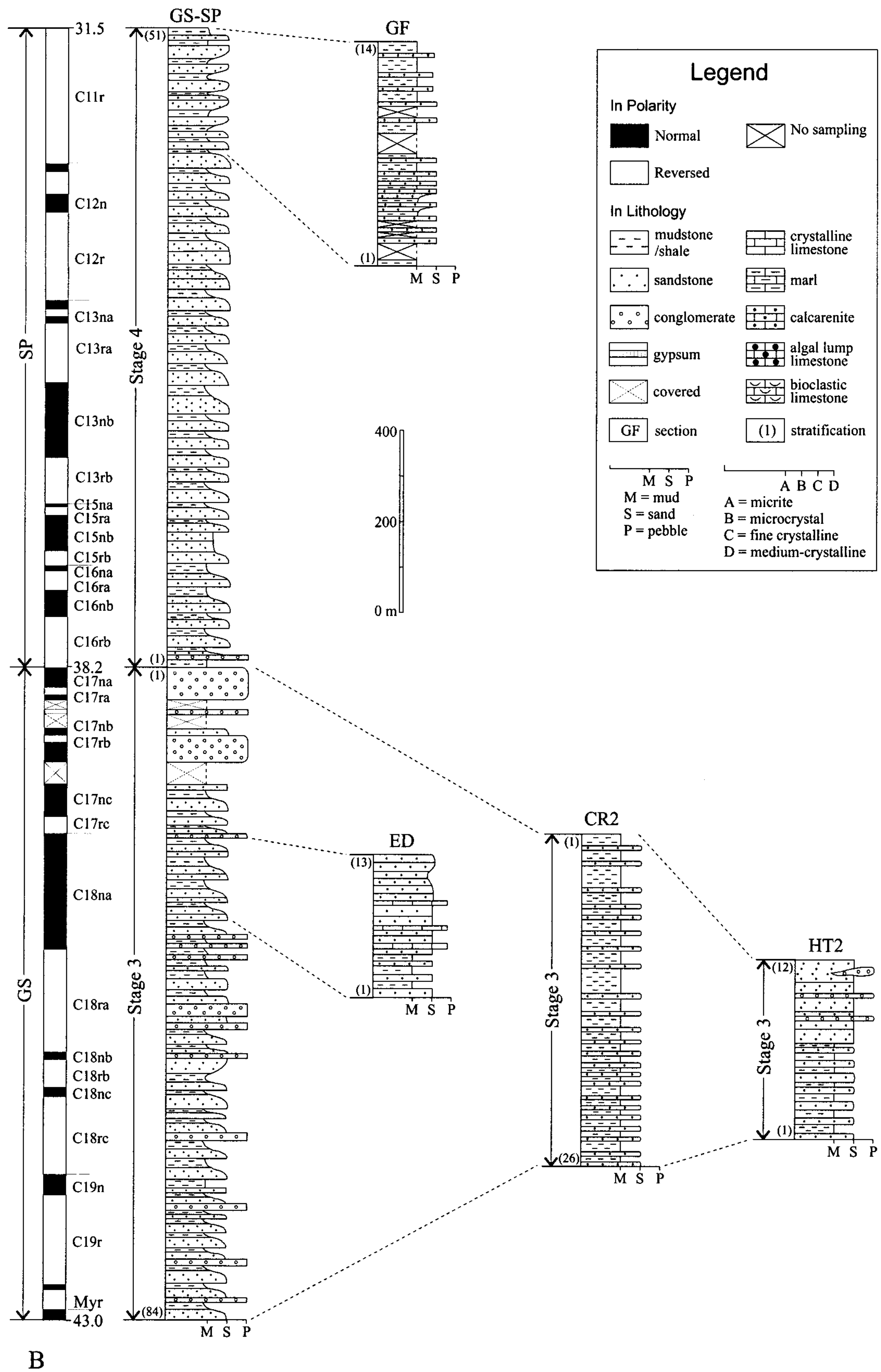

FIG. 3.—Continued.

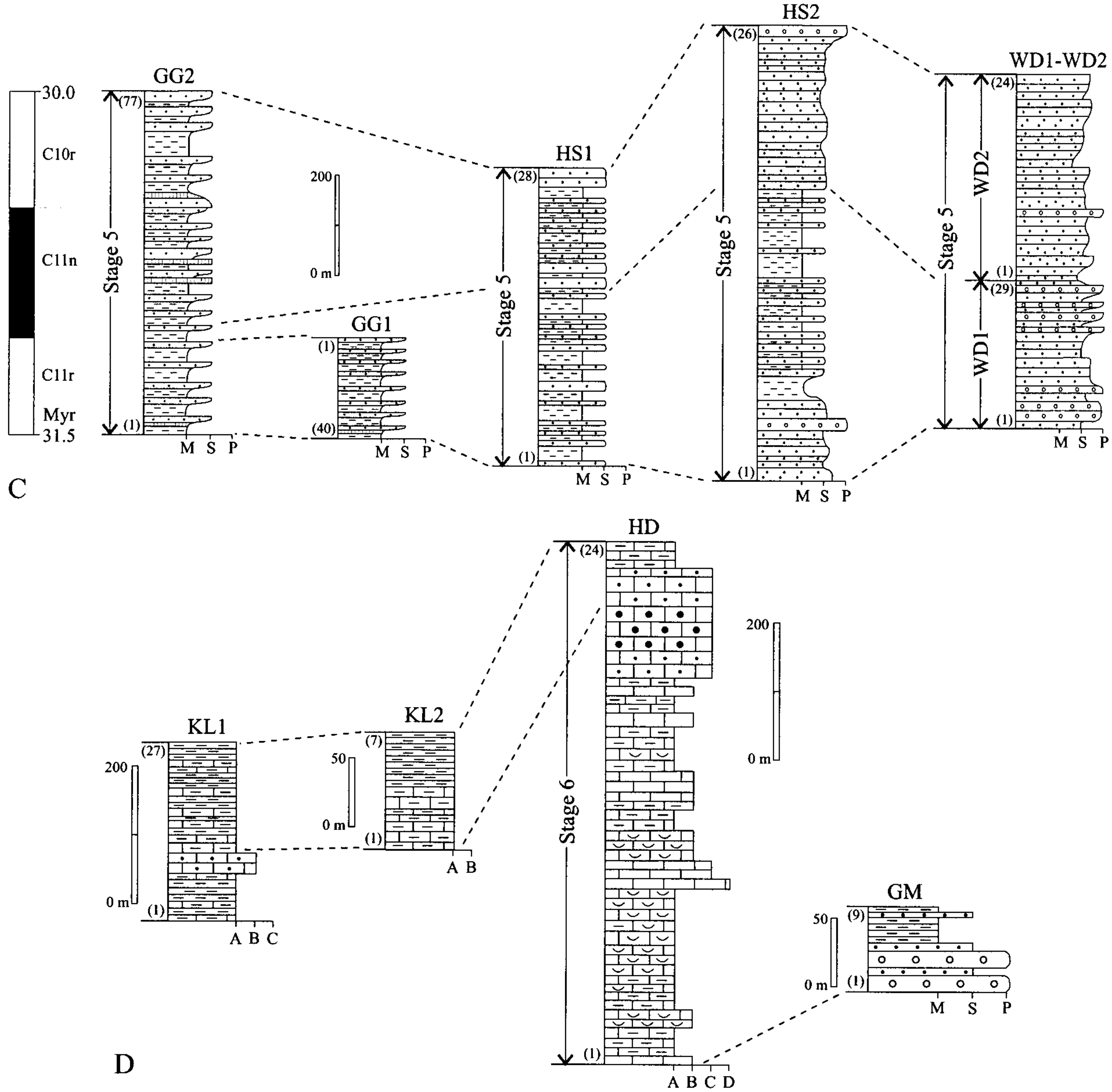

FIG. 3.—Continued.

the Bairizhajia Mountains and shows that thrusting moved northward in the foreland. In the southern Hoh Xil basin, sedimentation proceeded only in the Fenghuoshan sub-basin, with sediments 1,530 m thick. Paleocurrents were directed to the north in the southern part and to the east in the northern part.

From 31.5 to 30.0 Myr, during stage 5, sedimentation occurred mainly in the Wudaoliang sub-basin, with several depositional patches in the Fenghuoshan sub-basin to the south and the Zhuolai Lake sub-basin to the north (Fig. 4E). Paleocurrent directions in the Fenghuoshan sub-basin were to the north, whereas they were to the northeast and northwest in the Wudaoliang sub-basin. The patterns of the paleocurrents indicate that longitudinal filling occurred in the Wudaoliang sub-basin and latitudinal filling in the Fenghuoshan sub-basin.

From 30.0 Myr to the Early Miocene (~ 23.0 Myr), between stage 5 and stage 6, no sediment records have been found in the Hoh Xil basin. Sediments of the Fenghuoshan and Yaxicuo groups were thrusted and fold-

→

FIG. 4.—Reconstruction of the depositional history of the Cenozoic Hoh Xil basin, showing areal distribution, sediment thickness, and paleocurrent directions of Cenozoic sediments, development of sub-basins, and tectonic thrusting during six stages from the Early Eocene to the Early Miocene, with a period of sedimentation hiatus in the Late Oligocene. **A)** Stage 1: 56.0–52.0 Myr; **B)** stage 2: 52.0–43.0 Myr; **C)** stage 3: 43.0–38.2 Myr; **D)** stage 4: 38.2–31.5 Myr; **E)** stage 5: 31.5–30.0 Myr; **F)** stage 6: ~ 23.0 to ~ 16.0 Myr. Sedimentary isopachs were reconstructed by the interpolated point method based on corrected stratigraphic thickness with a calculation uncertainty of 15% and distribution of Cenozoic sediments. The distribution of present outcrops is assumed to represent the original depositional ranges. In rose plots of paleocurrent directions the arrows represent vector means. Other symbols are as in Figure 1.

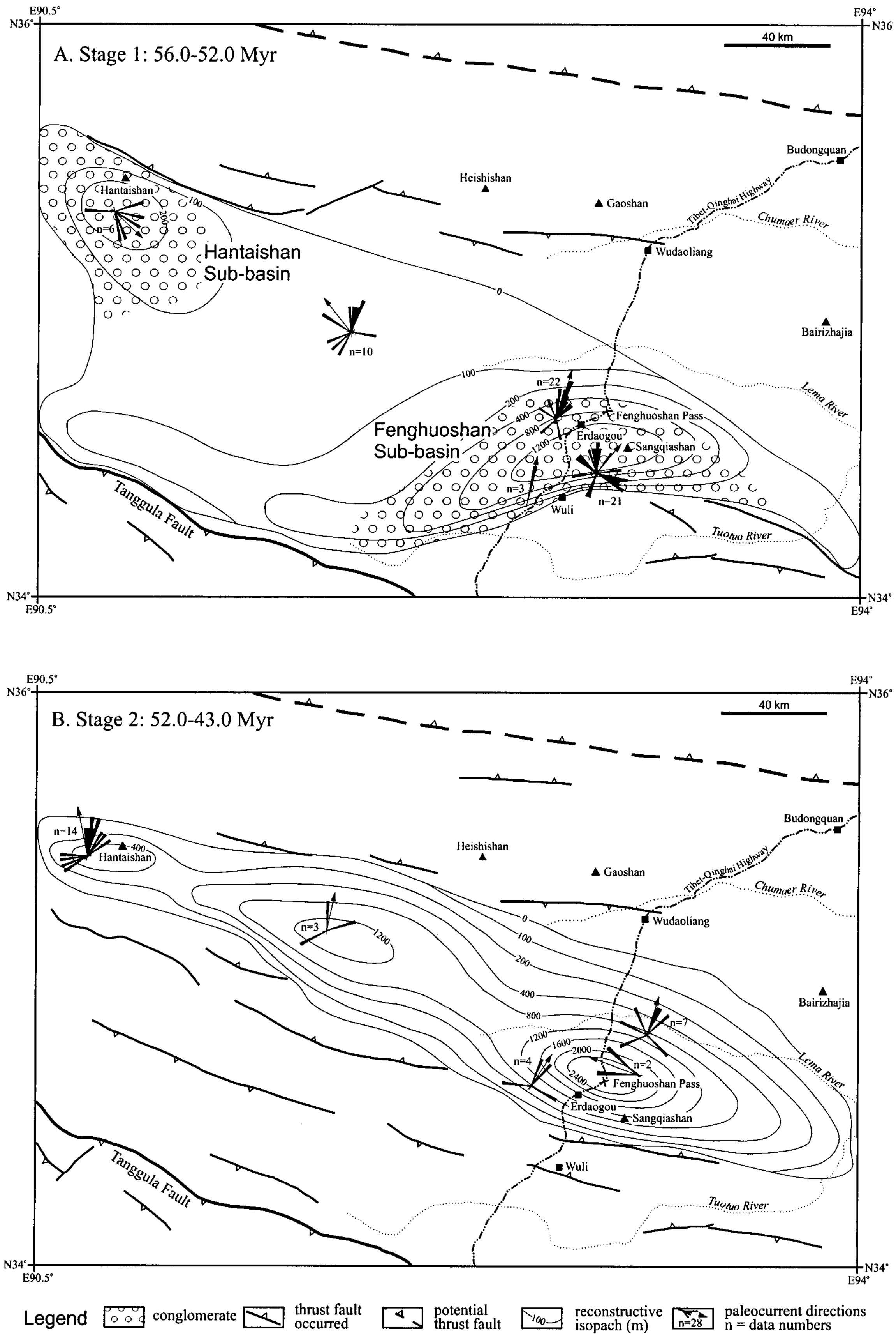
A. Stage 1: 56.0-52.0 Myr
E90.5°
N36°
E94°
N36°
40 km
Hantaishan
Hantaishan Sub-basin
n=6
100
200
Heishishan
Gaoshan
Budongquan
Tibet-Qinghai Highway
Chumaer River
Wudaoliang
0
n=10
Bairizhajia
Lema River
n=22
Fenghuoshan Pass
Fenghuoshan Sub-basin
Erdaogou
Sangqiashan
n=3
n=21
Wuli
Tanggula Fault
Tuotuo River
N34°
E90.5°
N34°
E94°
B. Stage 2: 52.0-43.0 Myr
E90.5°
N36°
E94°
N36°
40 km
n=14
400
Hantaishan
Heishishan
Gaoshan
Budongquan
Tibet-Qinghai Highway
Chumaer River
Wudaoliang
n=3
1200
0
100
200
400
800
Bairizhajia
n=7
1200
1600
2000
n=4
n=2
2400
Fenghuoshan Pass
Erdaogou
Sangqiashan
Lema River
Wuli
Tanggula Fault
Tuotuo River
N34°
E90.5°
N34°
E94°
Legend
conglomerate
thrust fault occurred
potential thrust fault
reconstructive isopach (m)
paleocurrent directions n = data numbers
n=28

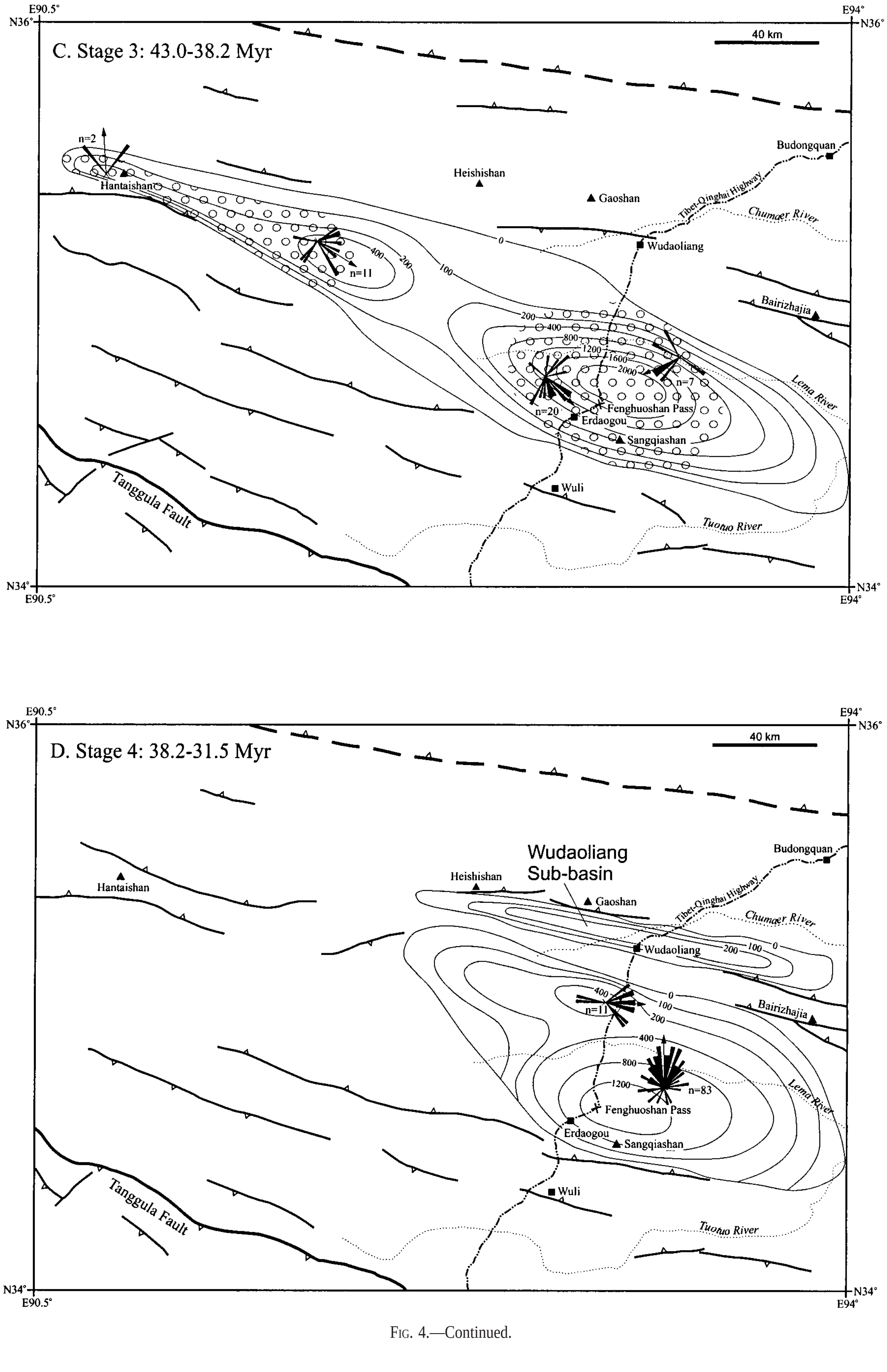

FIG. 4.—Continued.

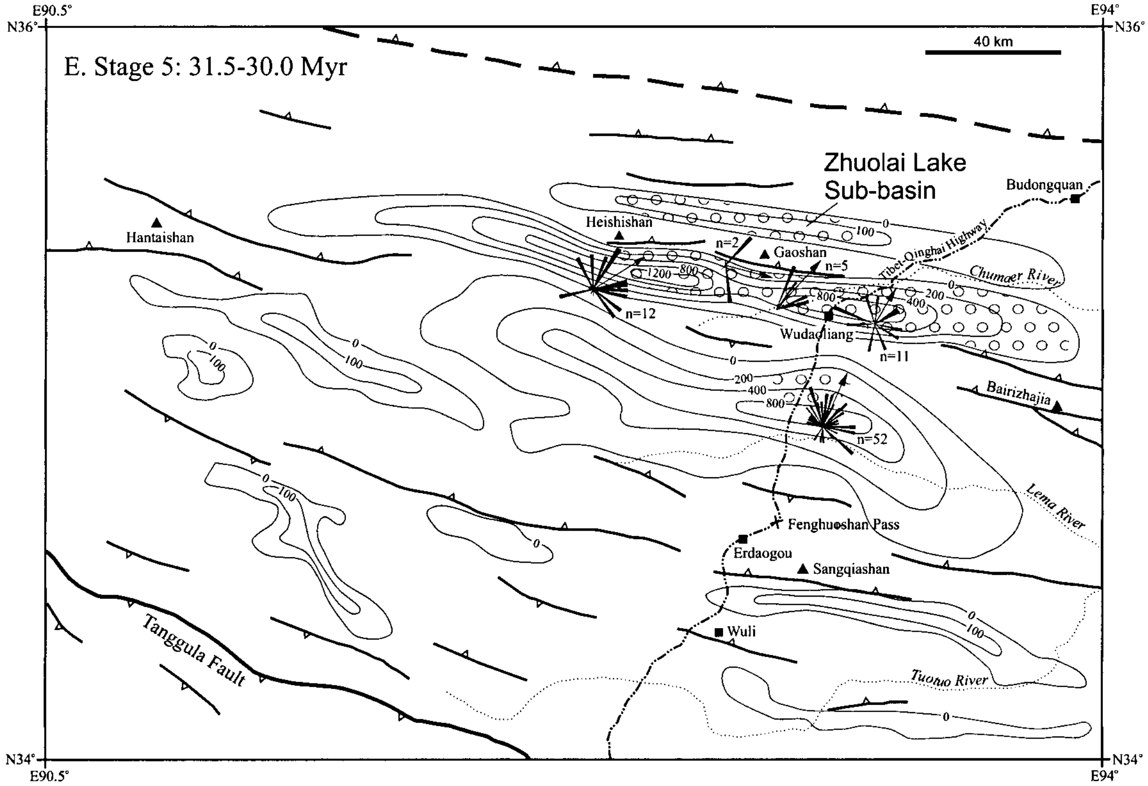

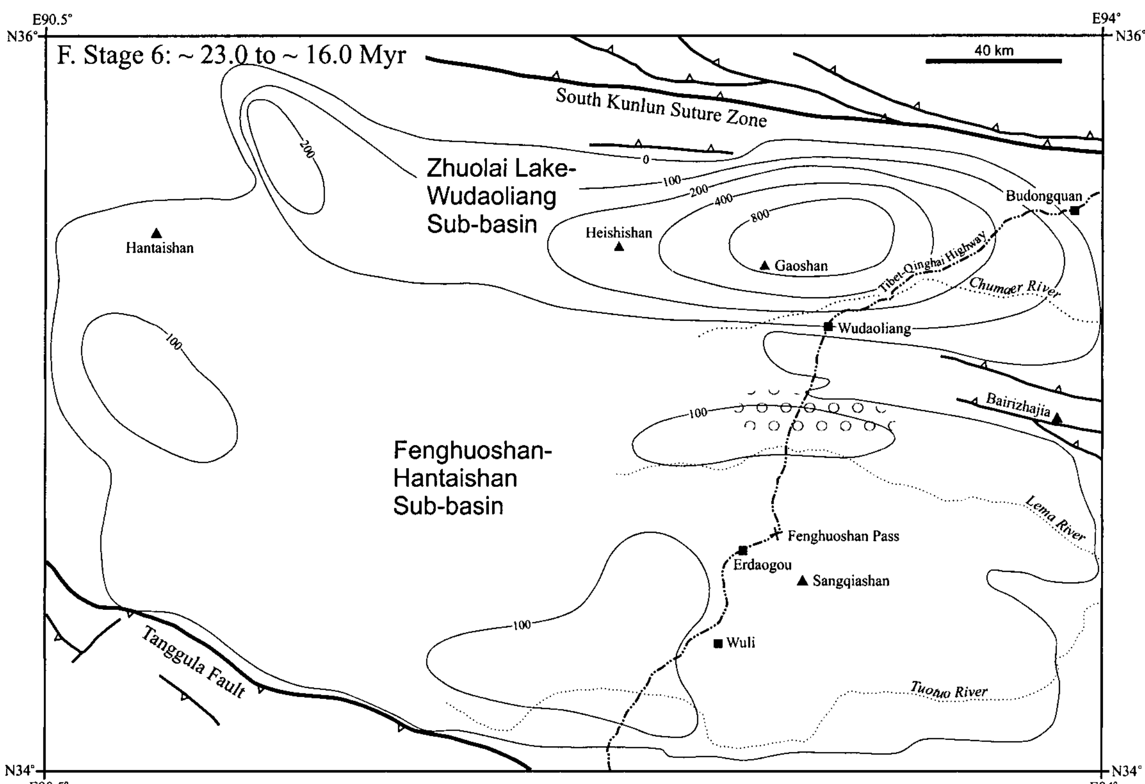

FIG. 4.—Continued.

TABLE 2.—*Data list for analyses of decompaction and mass accumulation of the Fenghuoshan and Yaxicuo groups on the basis of polarity chrons and sub-basins in the Hoh Xil basin, northern Tibet.*

Stratigraphy	Basin Evolution	Polarity Chrons	Ages (Myr)	Deposition Time (Myr)	Fenghuoshan sub-basin Thickness (m)	Depth (m)	c (km^{-1})	ϕ_0	ρ_{sg} (kg m^{-3})	Decompacted Thickness (m)	Restored Area (km^2)	Volume (km^3)	Wudaoliang sub-basin Thickness (m)	Depth (m)	c (km^{-1})	ϕ_0	ρ_{sg} (kg m^{-3})	Decompacted Thickness (m)	Restored Area (km^2)	Volume (km^3)
			~30.0			0								0						
Yaxicuo Group	Stage 5	C10r	30.42	0.42	221	221	0.44	0.59	2 699	221	14 064	3 108	310	310	0.27	0.48	2 645	310	4 972	1 541
		C11n	31.21	0.79	261	482	0.43	0.58	2 696	290	14 064	4 079	410	720	0.39	0.56	2 685	460	4 972	2 287
		C11r	31.60	0.39	471	953	0.39	0.56	2 685	555	14 064	7 806	672	1 392	0.36	0.55	2 680	818	4 972	4 067
	Stage 4	C12n	32.01	0.41	95	1 048	0.34	0.53	2 671	124	13 508	1 675	65	1 457	0.34	0.53	2 671	92	2 632	457
		C12r	34.26	2.25	211	1 259	0.34	0.53	2 671	277	13 508	3 742	120	1 577	0.34	0.53	2 671	171	2 632	850
		C13na	34.44	0.18	45	1 304	0.35	0.54	2 675	64	13 508	865								
		C13ra	34.50	0.06	132	1 436	0.35	0.54	2 675	186	13 508	2 512								
		C13nb	34.82	0.32	156	1 592	0.34	0.53	2 671	220	13 508	2 972								
		C13rb	36.12	1.30	113	1 705	0.35	0.54	2 675	167	13 508	2 256								
		C15na	36.32	0.20	7	1 712	0.34	0.53	2 671	10	13 508	135								
		C15ra	36.35	0.03	15	1 727	0.34	0.53	2 671	22	13 508	297								
		C15nb	36.54	0.19	77	1 804	0.34	0.53	2 671	115	13 508	1 553	Hantaishan sub-basin							
		C15rb	37.31	0.77	20	1 824	0.34	0.53	2 671	30	13 508	405	Thickness (m)	Depth (m)	c (km^{-1})	ϕ_0	ρ_{sg} (kg m^{-3})	Decompacted Thickness (m)	Restored Area (km^2)	Volume (km^3)
		C16na	37.58	0.27	31	1 855	0.35	0.54	2 675	48	13 508	648								
		C16ra	37.63	0.05	29	1 884	0.35	0.54	2 675	45	13 508	608								
		C16nb	38.01	0.38	40	1 924	0.35	0.54	2 675	62	13 508	837								
		C16rb	38.28	0.27	103	2 027	0.35	0.54	2 675	160	13 508	2 161								
Fenghuoshan Group	Stage 3	C17na	39.13	0.85	80	2 107	0.26	0.39	2 615	101	9 295	939		0						
		C17ra	39.20	0.07	13	2 120	0.26	0.39	2 615	16	9 295	149	47	47	0.26	0.39	2 615	47	9 295	437
		C17nb	39.39	0.19	15	2 135	0.26	0.39	2 615	19	9 295	177								
		C17rb	39.45	0.06	35	2 170	0.26	0.39	2 615	44	9 295	409								
		C17nc	39.77	0.32	222	2 392	0.26	0.40	2 619	283	9 295	2 630	127	174	0.26	0.40	2 619	128	9 295	1 190
		C17rc	39.94	0.17	32	2 424	0.35	0.54	2 675	53	9 295	493								
		C18na	40.36	0.42	251	2 675	0.31	0.49	2 655	369	9 295	3 430	208	382	0.30	0.48	2 651	217	9 295	2 017
		C18ra	40.43	0.07	225	2 900	0.30	0.48	2 651	333	9 295	3 095								
		C18nb	40.83	0.40	20	2 920	0.30	0.48	2 651	31	9 295	288	34	416	0.39	0.56	2 685	40	9 295	372
		C18rb	40.90	0.07	58	2 978	0.33	0.53	2 668	98	9 295	911								
		C18nc	41.31	0.41	16	2 994	0.33	0.53	2 668	27	9 295	251	82	498	0.30	0.48	2 615	91	9 295	846
		C18rc	42.14	0.83	171	3 165	0.32	0.50	2 659	271	9 295	2 519								
		C19n	42.57	0.43	45	3 210	0.34	0.52	2 666	77	9 295	716	95	593	0.39	0.56	2 685	115	9 295	1 069
		C19r	43.13	0.56	251	3 461	0.34	0.52	2 666	417	9 295	3 876								
	Stage 2	C20n	44.57	1.44	156	3 617	0.40	0.57	2 689	300	11 575	3 473	98	691	0.39	0.56	2 685	123	11 575	1 424
		C20r	47.01	2.44	111	3 728	0.43	0.58	2 696	225	11 575	2 604	70	761	0.39	0.56	2 685	90	11 575	1 042
		C21n	48.51	1.50	566	4 294	0.41	0.57	2 692	1023	11 575	11 841	356	1 117	0.37	0.55	2 678	449	11 575	5 197
		C21r	50.03	1.52	38	4 332	0.46	0.60	2 706	86	11 575	995	107	1 224	0.37	0.55	2 678	149	11 575	1 725
		C22n	50.66	0.63	132	4 464	0.45	0.60	2 703	290	11 575	3 357								
		C22r	51.85	1.19	34	4 498	0.44	0.59	2 699	75	11 575	868	325	1 549	0.39	0.56	2 685	462	11 575	5 348
		C23na	52.08	0.23	216	4 714	0.41	0.57	2 692	434	11 575	5 024								
	Stage 1	C23ra	52.13	0.05	113	4 827	0.37	0.55	2 678	222	17 561	3 899	39	1 588	0.27	0.49	2 650	52	17 561	913
		C23nb	52.83	0.70	25	4 852	0.44	0.59	2 699	56	17 561	983								
		C23rb	53.39	0.56	108	4 960	0.44	0.59	2 699	237	17 561	4 162	74	1 662	0.27	0.46	2 641	96	17 561	1 686
		C24na	53.69	0.30	82	5 042	0.33	0.53	2 668	154	17 561	2 704								
		C24ra	54.05	0.36	209	5 251	0.34	0.53	2 671	388	17 561	6 814	88	1 750	0.25	0.38	2 612	106	17 561	1 686
		C24nb	54.65	0.60	45	5 296	0.32	0.52	2 664	84	17 561	1 475								
		C24rb	~56.0	1.35	157	5 453	0.37	0.55	2 678	312	17 561	5 479	54	1 804	0.25	0.35	2 603	64	17 561	1 124

Polarity chrons and ages are modified from Liu et al. (2000a) according to the timescale of Harland et al. (1990) and the method of decompation analysis is after Allen and Allen (1990) and Shao et al. (1999). Areas of sub-basins are restored according to the north-south crustal shortening of 42.8% after Wang et al. (1999). The calculation uncertainty is about 5% for thickness and depth, 15% for decompacted thickness and restored area, and 30% for volume. c, depth coefficient; ϕ_0, surface porosity; ρ_{sg}, density (Sclater and Christie 1980; Allen and Allen 1990; Shao 1996).

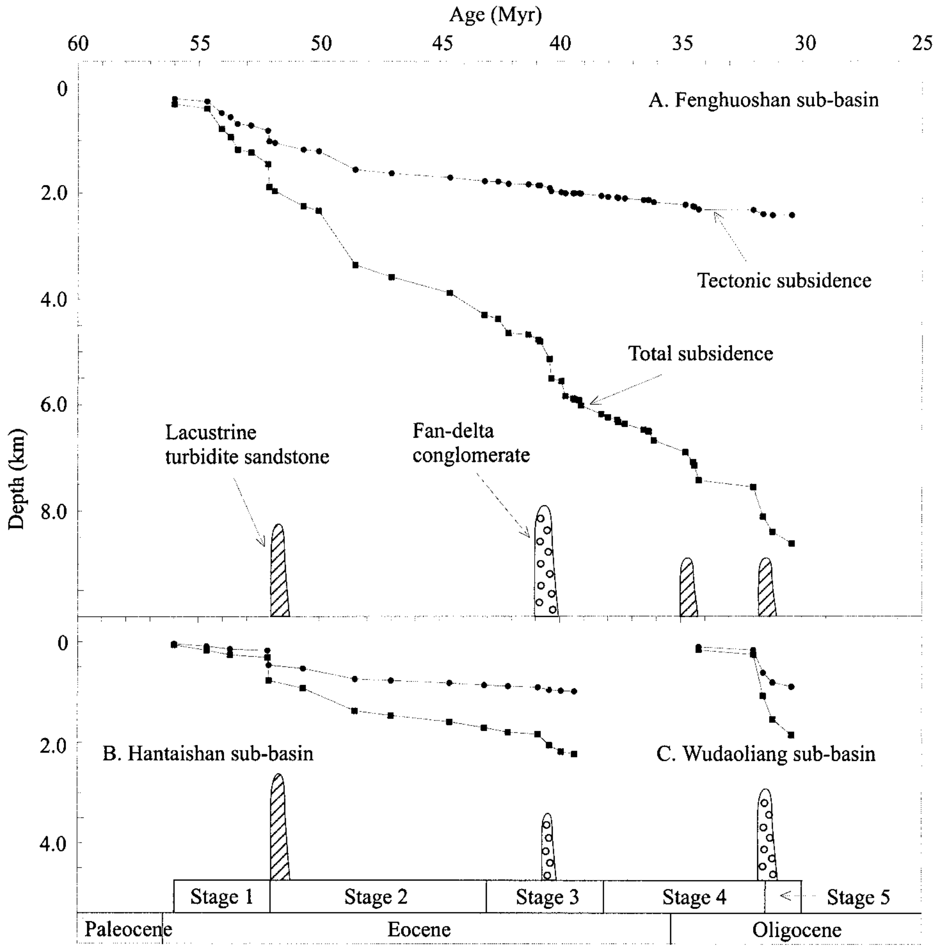

FIG. 5.—Curves of subsidence history for three sub-basins in the Hoh Xil basin, showing that the sub-basins underwent only flexure subsidence during the Paleogene. **A)** The Fenghuoshan sub-basin; **B)** the Hantaishan sub-basin; **C)** the Wudaoliang sub-basin. There are four accelerated subsidence periods associated with the occurrence of lacustrine turbidite sandstone and fan-delta conglomerate according to analysis of depositional systems (Liu and Wang 2001). The calculation uncertainty of decompacted depth is about 15%.

ed. The tectonic uplift caused 42.8% north–south crustal shortening in the Fenghuoshan–Wudaoliang areas (Wang et al. 1999). In the Early Miocene (~ 23.0 to ~ 16.0 Myr), during stage 6, the Wudaoliang Group developed throughout the entire Hoh Xil basin, with the depocenter in the Zhuolai Lake–Wudaoliang sub-basins, where over 800 m of sediments accumulated (Fig. 4F). Only thinly stratified but widely distributed limestone was deposited in the Fenghuoshan–Hantaishan sub-basins. The limestone of the Wudaoliang Group has undergone only weak deformation with minor tilting since then.

In summary, the Cenozoic sediments in the Hoh Xil basin become gradually younger and thinner from southwest to northeast, indicating northeastward tectonic movement. The depocenters of sub-basins, areas of greatest thickness of isopachs, occurred just in front of the thrusts (Fig. 4). They moved mainly eastward and northward as indicated by paleocurrent data. Therefore, during the Eocene and Early Oligocene, when the Fenghuoshan and Yaxicuo groups were developed, the Hoh Xil basin was formed and filled on northeastward-moving thrust sheets that have been described as piggyback basins (Liu et al. 2000b). The Hoh Xil piggyback basins coincide well with the mechanism of northeastward growth of the Tibetan Plateau, first proposed on the basis of research on the Qaidam and Hexi Corridor and adjacent mountains at the northeastern margin of the plateau (Meyer et al. 1998; Métivier et al. 1998). Therefore, this study supports the mechanism of intracontinental subduction and northeastward growth and places the onset of northeastward growth of central Tibet from the Early Eocene (about 56 Myr) to the Late Oligocene.

Subsidence History and Accumulation Rate

From the decompaction of the stratigraphic thickness and the analysis of basin evolution, we construct the subsidence history using corrected thickness after the method of Allen and Allen (1990) and Shao et al. (1999) and assess the sediment accumulation according to the hypothesis of regional similarity developed by Métivier and Gaudemer (1997) and Métivier et al. (1998) on the units of polarity chrons and sub-basins (Table 2).

Figure 5 includes curves of total subsidence and tectonic subsidence of three sub-basins in the Hoh Xil basin during the Paleogene. The total subsidence of the Fenghuoshan sub-basin was more than 8 km from the Early Eocene to the Early Oligocene with four periods of accelerated subsidence at about 52.0, 40.5, 34.5, and 31.5 Myr (Fig. 5A). According to an analysis of the depositional systems (Liu and Wang 2001), lacustrine turbidite sandstones were deposited at 52.0, 34.5, and 31.5 Myr, whereas fan-delta conglomerate was deposited at 40.5 Myr in the Fenghuoshan sub-basin. The Hantaishan sub-basin developed total subsidence of about 2 km in the Eocene with two periods of rapid subsidence at 52.0 and 40.5 Myr (Fig. 5B). The two episodes of rapid subsidence coincide with a lacustrine turbidite sandstone and a fan-delta conglomerate, respectively (Liu and Wang 2001).

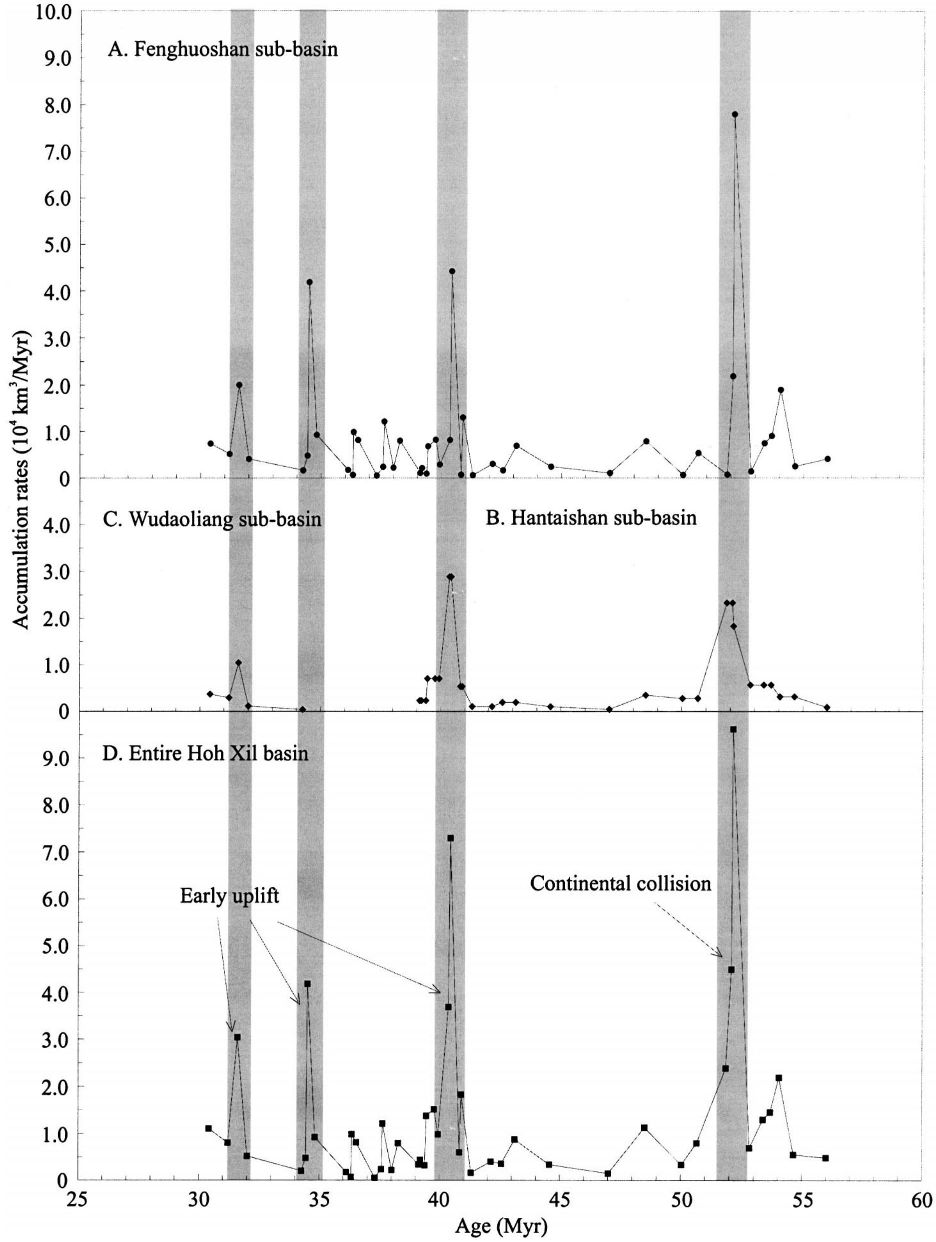

FIG. 6.—Curves of accumulation rate of Cenozoic sediments for three sub-basins and the entire Hoh Xil basin, indicating four periods of sudden increases of accumulation rates during the Paleogene. **A)** The Fenghuoshan sub-basin; **B)** the Hantaishan sub-basin; **C)** the Wudaoliang sub-basin; **D)** the entire Hoh Xil basin. The sudden increase at 52.0 Myr may represent the continental collision between India and Asia, whereas the other three increases during about 40–30 Myr may show the early uplift of the Tibetan Plateau. The calculation uncertainty of accumulation rates is about 30%.

In the Wudaoliang sub-basin, although the depositional time was short (about 4 Myr), subsidence accelerated at 31.5 Myr and total subsidence reached nearly 2 km (Fig. 5C). The subsidence coincides well with presence of a fan-delta conglomerate (Liu and Wang 2001). The synchronization between the curves of total subsidence and tectonic subsidence, along with the analysis of the basin evolution and depositional systems, indicates that the subsidence of the Hoh Xil basin during the Paleogene was controlled by tectonic movement.

Figure 6 shows the accumulation rate curves for the three sub-basins and the entire Hoh Xil basin. As with the subsidence curves in Fig. 5, the accumulation rates show four peaks in the Fenghuoshan sub-basin (Fig. 6A), two peaks in the Hantaishan sub-basin (Fig. 6B), and one peak in the Wudaoliang sub-basin (Fig. 6C). The accumulation rate of the entire basin is up to near 10.0×10^4 km^3/Myr at 52.0 Myr, to over 7.0×10^4 km^3/Myr at 40.5 Myr, and to near 4.0×10^4 km^3/Myr at 34.5 Myr and 31.5 Myr. Therefore, the sudden increase of accumulation rates in the Cenozoic Hoh Xil basin took place at the same time as the accelerated subsidence and the onset of deposition of lacustrine turbidite sandstone and fan-delta conglomerate, which resulted from the northeastward tectonic movement.

On the basis of the mechanism of northeastward growth of the piggyback basins (Liu et al. 2000b) and the consistency of accelerated subsidence and mass accumulation, we suggest that the tectonic–sedimentary events recorded in the Hoh Xil basin may have a direct relationship to the continental collision and early uplift of the Tibetan Plateau. The most sudden increase of accumulation rates at 52.0 Myr could represent the continental collision between India and Asia (Fig. 6). This age is consistent with some reported collision ages (e.g., Patriat and Achache 1984; Richter et al. 1992). The other three increases of accumulation rates during about 40–30 Myr may show the early uplift of the Tibetan Plateau (Fig. 6). We find that the ages of the early uplift recorded in the Hoh Xil basin coincide well with the widespread distribution of potassic lavas that formed in northern Tibet. The present high elevation and extensional deformation of the Tibetan Plateau probably resulted from convective thinning of the underlying lithospheric mantle (England and Houseman 1989). Potassic lavas related to the convective thinning have been regarded as an indicator of rapid uplift of the Tibetan Plateau. The widespread magmatic activity began at about 40 Myr in eastern Tibet (Chung et al. 1998) and at 20 Myr in the west (Turner et al. 1993). Correlation between magmatic activity in the east and west, and the sedimentary record of the Hoh Xil basin in the center, suggest a diachronous uplift history for the Tibetan Plateau from east to west (Chung et al. 1998).

CONCLUSIONS

This paper presents an attempt to reconstruct the depositional history and to calculate the mass stored in the Cenozoic Hoh Xil basin, northern Tibet, on the basis of measured stratigraphic sections. We applied the backstripping method to correct the measured stratigraphic thickness, and simple geometric hypotheses of regional similarity of the strata on the basis of sub-basins and the interpolated isopach distribution to obtain a conservative estimate of the mass that accumulated in the Hoh Xil basin during the Paleogene.

The results show that the Hoh Xil basin underwent six stages of development from 56.0 to ∼ 16.0 Myr, with a hiatus in sedimentation in the Late Oligocene. During the first five stages, between 56.0 to 30.0 Myr, the continuous Fenghuoshan and Yaxicuo groups developed, and basin depocenters moved eastward and northward along with the direction of migration of thrusting. During the last stage of ∼ 23.0 to ∼ 16.0 Myr, the Wudaoliang Group was deposited spread the entire basin. The strata of the Fenghuoshan and Yaxicuo groups underwent strong deformation, mainly during the Late Oligocene, whereas only minor tilting has occurred in the Wudaoliang Group since then. The evolution of the Hoh Xil basin indicates that the basin was formed as a series of piggyback basins and that the onset of northeastward growth of central Tibet was from the Early Eocene (about 56 Myr) to the Late Oligocene.

Analysis of the subsidence history of three sub-basins indicates that four periods of accelerated subsidence took place at about 52.0, 40.5, 34.5, and 31.5 Myr from the Early Eocene to the Early Oligocene. During the four periods, lacustrine turbidite sandstones or fan-delta conglomerates were deposited as a result of the northeastward tectonic movement. Moreover, the mass accumulation rates of the three sub-basins and of the entire basin show four sudden increases, which took place at the same time as the four periods of accelerated subsidence. On the basis of the mechanism of northeastward growth of the piggyback basins and the consistency of accelerated subsidence, the nature of the depositional systems, and mass accumulation, we suggest that the continental collision and early uplift of the Tibetan Plateau controlled the formation and evolution of the Hoh Xil basin. The event that occurred at 52.0 Myr may represent the continental collision between India and Asia, whereas the other three events, which happened during about 40–30 Myr, may indicate the early uplift of the Tibetan Plateau. This study on the sedimentary record in the Hoh Xil basin, along with widespread magmatic activity in the eastern and western Tibet, suggests a diachronous uplift history for the Tibetan Plateau from east to west.

ACKNOWLEDGMENTS

We are grateful to Dr. Shun Liu, Dr. Xianghui Li, Xiumian Hu, Lidong Zhu, and Shifeng Wang for help in the field, to Dr. Xixi Zhao for magnetostratigraphic analysis, to Dr. Lei Shao for help in subsidence analysis, and to Prof. Pinxian Wang and Dr. Hongbo Zheng for helpful comments. We are also thankful to Dr. Réjean Hébert for improving the readability and consistency of this paper. We specially thank Prof. Karl Stattegger, Dr. Brian D. Ricketts, Dr. Mary J. Kraus, and one anonymous reviewer for their encouragement and constructive reviews that significantly helped to improve this work. This study was supported by the NKBRSF Project of China (1998040800), the Outstanding Youth Scientific Foundation of China (40025107), the Ninth Five-Year Project of Ministry of Land and Resource of China (9501101-02), and Post-Doctor Science Foundation of China.

REFERENCES

Allen, P.A., and Allen, J.R., 1990, Basin Analysis: Principles and Applications: Oxford, U.K., Blackwell, 443 p.

Bureau of Geology and Mineral Resources of Qinghai, 1987, Regional geologic survey report on Wenquan, scale 1:200,000: Xining, Bureau of Geology and Mineral Resources of Qinghai, 350 p.

Bureau of Geology and Mineral Resources of Qinghai, 1991, Regional geology of Qinghai: Beijing, Geological Press, 662 p.

Chung, S., Lo, C., Lee, T., Zhang, Y., Xie, Y., Li, X., Wang, K., and Wang, P., 1998, Diachronous uplift of the Tibetan Plateau starting 40 Myr ago: Nature, v. 394, p. 769–773.

Coward, W.P., Kidd, W.S.F., Pang, Y., Shackleton, R.M., and Zhang, H., 1990, The structure of 1985 Tibet Geotraverse, Lhasa to Golmud, *in* Sino-British Comprehensive Geological Expedition Team of the Qinghai-Tibet Plateau, ed., The Geological Evolution of the Qinghai-Tibet: Beijing, Science Press, p. 321–347.

England, P., and Houseman, G., 1989, Extension during continental convergence, with application to the Tibetan Plateau: Journal of Geophysical Research, v. 94, p. 17561–17579.

Harland, W.B., Armstrong, R.L., Cox, A.V., Craig, L.E., Smith, A.G., and Smith, D.G., 1990, A Geologic Time Scale 1989: Cambridge, U.K., Cambridge University Press, 263 p.

Hay, W.W., Shaw, C.A., and Wold, C.N., 1989, Mass-balanced paleogeographic reconstructions: Geologische Rundschau, v. 78, p. 207–242.

Jaeger, J.J., Courtillot, V., and Tapponnier, P., 1989, Paleontological view of the ages of the Deccan Traps, the Cretaceous/Tertiary boundary and the India–Asia collision: Geology, v. 17, p. 316–319.

Kutzbach, J.E., Prell, W.L., and Ruddiman, W.F., 1993, Sensitivity of Eurasian climate to surface uplift of the Tibetan Plateau: Journal of Geology, v. 101, p. 177–190.

Liu, Z., and Wang, C., 1999, Oil shale in the Tertiary Hoh Xil Basin, northern Qinghai–Tibet Plateau: American Association of Petroleum Geologists, Bulletin, v. 83, p. 1890.

Liu, Z., and Wang, C., 2000, Depositional environment and paleoclimatic significance of the Early Oligocene Yaxicuo Group in the Hoh Xil Basin: Acta Sedimentologica Sinica, v. 18 (3), p. 355–361.

Liu, Z., and Wang, C., 2001, Facies analysis and depositional systems of Cenozoic sediments in the Hoh Xil Basin, northern Tibet: Sedimentary Geology, v. 140, p. 251–270.

Liu, Z., Wang, C., Zhao, X., Liu, S., and Yi, H., 2000a, Magnetostratigraphic dating: Implications for Tertiary evolution of the Hoh Xil basin, northern Tibet (abstract): 15th Himalaya–Karakoram–Tibet Workshop Abstracts, Earth Science Frontiers, v. 7 (Supplement), p. 157–159.

Liu, Z., Wang, C., Yi, H., and Liu, S., 2000b, Hoh Xil piggyback basins: Implications for Paleogene shortening of the Tibetan Plateau (abstract): 15th Himalaya–Karakoram–Tibet Workshop Abstracts, Earth Science Frontiers, v. 7 (Supplement), p. 152–153.

Métivier, F., and Gaudemer, Y., 1997, Mass transfer between eastern Tien Shan and adjacent basins (central Asia): constraints on regional tectonics and topography: Geophysical Journal International, v. 128, p. 1–17.

Métivier, F., Gaudemer, Y., Tapponnier, P., and Klein, M., 1999, Mass accumulation rates in Asia during the Cenozoic: Geophysical Journal International, v. 137, p. 280–318.

Métivier, F., Gaudemer, Y., Tapponnier, P., and Meyer, B., 1998, Northeastward growth of the Tibet Plateau deduced from balanced reconstruction of two depositional areas: The Qaidam and Hexi Corridor basins, China: Tectonics, v. 17, p. 823–842.

Meyer, B., Tapponnier, P., Bourjot, L., Métivier, F., Gaudemer, Y., Peltzer, G., Guo, S., and Chen, Z., 1998, Crustal thickening in Gansu–Qinghai, lithospheric mantle subduction, and oblique, strike-slip controlled growth of the Tibet Plateau: Geophysical Journal International, v. 135, p. 1–47.

Patriat, P., and Achache, J., 1984, India–Eurasia collision chronology has implications for crustal shortening and driving mechanism of plates: Nature, v. 311, p. 615–621.

Rage, J.C., Cappetta, H., Hartenberger, J.L., Jaeger, J.J., Sudre, J., Vianeyliaud, M., Kumar, K., Prasad, G.V.R., and Sahnl, A., 1995, Collision age: Nature, v. 375, p. 286.

Richter, F., Rowley, D.B., and DePaolo, D.J., 1992, Sr isotope evolution of seawater: The role of tectonics: Earth and Planetary Science Letters, v. 109, p. 11–23.

Rowley, D.B., 1998, Minimum age of initiation of collision between India and Asia North of Everest based on the subsidence history of the Zhepure Mountain section: Journal of Geology, v. 106, p. 229–235.

Ruddiman, W.F., and Kutzbach, J.E., 1991, Plateau uplift and climatic change: Scientific American, v. 264, p. 66–75.

Ruddiman, W.F., Raymo, M.E., Prell, W.L., and Kutzbach, J.E., 1997, The uplift–climate connection: A synthesis, *in* Ruddiman, W.F., ed., Tectonic Uplift and Climate Change: New York and London, Plenum Press, p. 471–515.

Sclater, J.G., and Christie, P.A.F., 1980, Continental stretching: An explanation of the post-mid-Cretaceous subsidence of the central North Sea Basin: Journal of Geophysical Research, v. 85, p. 3711–3739.

Shao, L., 1996, Sedimentology and evolution of the Turpan Basin (NW China): Institute Report of Geologic and Paleontologic Institute 80: Kiel, Germany, Kiel University Press, p. 102–106.

Shao, L., Stattegger, K., Li, W., and Haupt, B.J., 1999, Depositional style and subsidence history of the Turpan Basin (NW China): Sedimentary Geology, v. 128, p. 155–169.
Steckler, M.S., and Watts, A.B., 1978, Subsidence of the Atlantic-type continental margin off New York: Earth and Planetary Science Letters, v. 41, p. 1–13.
Tapponnier, P., Mattauer, M., Proust, F., and Cassaigneau, C., 1981, Mesozoic ophiolites, sutures and large scale tectonic movements in Afghanistan: Earth and Planetary Science Letters, v. 97, p. 355–371.
Turner, S., Hawkesworth, C., Liu, J., Rogers, N., Kelly, S., and van Calsteren, P., 1993, Timing of Tibetan uplift constrained by analysis of volcanic rocks: Nature, v. 364, p. 50–54.
van Hinte, J.E., 1978, Geohistory analysis—Application of micropaleontology in exploration geology: American Association of Petroleum Geologists, Bulletin, v. 62, p. 201–222.
Wang, C., Liu, Z., Zhao, X., and Liu, S., 1999, Sedimentology of the Fenghuoshan Group in the Hoh Xil Basin, northern Qinghai–Tibet Plateau: Implication for the plateau uplift history (abstract): 14th Himalaya–Karakoram–Tibet Workshop Abstracts, Terra Nostra, v. 99, p. 166–167.
Yin, J., Xu, J., Liu, C., and Li, H., 1990, The Tibetan Plateau: regional stratigraphic contex and previous work, *in* Sino-British Comprehensive Geological Expedition Team of the Qinghai–Tibet Plateau, ed., The Geological Evolution of the Qinghai–Tibet: Beijing, Science Press, p. 1–48.
Zhang, Y., and Zheng, J., 1994, Geological survey of the Hoh Xil and adjacent regions in Qinghai province: Beijing, Seismology Press, 177 p.

Received 24 March 2000; accepted 9 March 2001.